

Neutron Diffraction Studies on the Hydrogen-Bonded Structure of Water Molecules in Ion Exchange Resins

Yasuo Kameda,*[1] Koji Yamanaka,[2] Motoya Sasaki,[1] Yuko Amo,[1] and Takeshi Usuki[1]

[1]Department of Material and Biological Chemistry, Faculty of Science, Yamagata University, Yamagata 990-8560

[2]R & D Center, Organo Corporation, Kanagawa 229-0012

Received October 21, 2005; E-mail: kameda@sci.kj.yamagata-u.ac.jp

Neutron diffraction measurements were carried out for anion and cation exchange resins (AER and CER, respectively) absorbing H/D isotopically substituted water molecules in order to obtain structural information on the hydrogen-bonded network among water molecules within the resins. Partial structure factors, $a_{HH}(Q)$, $a_{XH}(Q)$, and $a_{XX}(Q)$ (X: atoms involved in the sample except for water-hydrogen atom), for AER and CER samples were respectively deduced from combined analyses of intermolecular interference terms observed for resins containing D_2O (99.8% D), $^{0}H_2O$ (35.9% D), and $^{0-2}H_2O$ (67.9% D). The nearest neighbor distances, $r(O\cdots H) = 1.95(3)$ Å and $r(H\cdots H) = 2.40(3)$ Å, determined for the AER sample agree well with those reported for pure liquid water. On the other hand, considerably shorter intermolecular distances, $r(O\cdots H) = 1.78(3)$ Å and $r(H\cdots H) = 2.28(3)$ Å, were found for the CER sample, implying that the hydrogen-bonded network among water molecules in CER would be strongly affected by a highly acidic environment.

Ion exchange resins provide wide applications in extensive fields of fundamental and industrial chemical processes.[1,2] Considerable effort has been made to investigate the ion-exchanging mechanism within the resin, which is indispensable to improve its performance. Recently, the swelling behavior of sulfonated poly(styrene/divinylbenzene) cation exchange resins were examined by means of small angle neutron scattering.[3] The swelling property was found to be strongly correlated with the cross-linking density of the resin. No remarkable change associated with the swelling was observed in the microscopic structure within the order of tens to hundreds of angstroms.[3] The hydration structure of Ni^{2+} and Li^{+} in the divinylbenzene cross-linked poly(styrene/sulfonate) cation exchange resins has been reported by means of neutron diffraction with the isotopic substitution method.[4] An indication of a decrease in the number of water molecules in the first hydration shell of Ni^{2+} has been reported that suggests the presence of a strong interaction between Ni^{2+} and the sulfonate group in the resin.[4] More recently, local structures of Cl^{-} and Br^{-} in the anion exchange resin have been investigated by XAFS.[5] It has been found that the maximum hydration number of these anions is 3 when they are bound by the ion-exchanging group in the resin. Despite these efforts to elucidate structural properties of the ion exchange resins, no direct information concerning the hydrogen-bonded structure among water molecules in the resins has yet been obtained.

In the present paper, we describe the results of neutron diffraction measurements on divinylbenzene cross-linked polystylene based cation and anion exchange resins absorbing H/D isotopically substituted water molecules in order to obtain structural information on the hydrogen-bonded network among water molecules within the resins.

Experimental

Materials. Cation exchange resin (CER, AMBERLITE® IR124H, H^{+} form, divinylbenzene cross-linked poly(styrene/sulfonate)) and anion exchange resin (AER, AMBERLITE® IRA402BL, OH^{-} form, divinylbenzene cross-linked poly(styrene/trimethylammonium hydroxide)) both absorbing D_2O were prepared by soaking them into more than 10 times the molar quantity of D_2O (Kanto Chemical, 99.9% D) with respect to that of water molecules within the resins. After equilibration for 24 h, extraneous water outside the resin was then removed. This procedure was repeated 3 times. Weighed amounts of resins absorbing D_2O and H_2O were mixed to obtain resins involving water with an average D content of 35.9% ($^{0}H_2O$, the average scattering length of the hydrogen atom, b_H, is set to be 0) and 67.9% ($^{0-2}H_2O$, $b_H = b_D/2$). The water content inside the anion and cation exchange resins was determined to be 70.0 and 47.1%, respectively. These correspond to the stoichiometric representations, $(AER)_{0.0434}(^{*}H_2O)_{0.9566}$ and $(CER)_{0.1067}(^{*}H_2O)_{0.8933}$, where AER and CER stand for the average monomeric unit of anion and cation exchange resins, respectively. Dried resins were prepared by dehydration at 40 °C in a vacuum dryer for 10 h. Each sample resin was sealed in a cylindrical quartz cell (11.6 mm in inner diameter and 1.2 mm in thickness). The shape of the AER and CER resins was spherical with an average diameter of 0.5 mm, which implies that the number of resin beads exposed to the incident neutron beam in the present experimental condition is ca. 4500, considering the packing fraction of the wet resins, ≈0.56, obtained from the measurement of the apparent density. This ensures that the mixture of the D_2O and H_2O absorbed resins can be regarded as an isotopic mixture of H and D, and are adequate to use for deriving the partial structure factors. Sample parameters are summarized in Table 1.

Neutron Diffraction Measurements. The neutron diffraction measurements were carried out at 25 °C using an ISSP diffractometer 5G (PONTA) installed at the JRR-3M research reactor oper-

Published on the web July 4, 2006; doi:10.1246/bcsj.79.1032

Table 1. Isotopic Compositions, Mean Scattering Lengths, b_H, for Exchangeable Hydrogen Atom, Total Cross Sections, and the Number Densities Scaled at the Stoichiometric Unit, $(Resin)_x(^*H_2O)_{1-x}$, σ_t, and ρ, Respectively, for Samples Used in This Study

Samples	H/%	D/%	$b_H/10^{-12}$ cm[a)]	σ_t/barns[b)]	ρ/Å^{-3}
$(AER)_{0.0434}(D_2O)_{0.9566}$	0.2	99.8	0.666	49.12	
$(AER)_{0.0434}(^0H_2O)_{0.9566}$[c)]	64.1	35.9	0	84.81	0.02044
$(AER)_{0.0434}(^{0-2}H_2O)_{0.9566}$	32.1	67.9	0.333	66.94	
$(CER)_{0.1067}(D_2O)_{0.8933}$	0.2	99.8	0.666	43.21	
$(CER)_{0.1067}(^0H_2O)_{0.8933}$	64.1	35.9	0	81.43	0.02710
$(CER)_{0.1067}(^{0-2}H_2O)_{0.8933}$	32.1	67.9	0.333	62.29	

a) Taken from Ref. 6. b) Calculated using total cross sections of D_2O and H_2O[7,8] for the incident neutron wavelength of 1.089 Å. c) The superscript 0 denotes the isotopic mixture with $b_H = 0$.

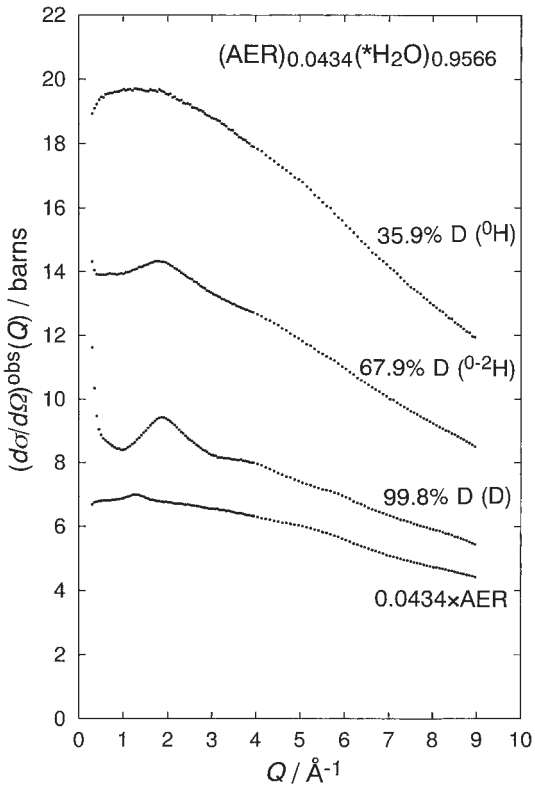

Fig. 1. Observed scattering cross sections, $(d\sigma/d\Omega)^{obs}$, for the anion exchange resin (AER) absorbed the water molecules with different H/D ratios of exchangeable hydrogen atoms and that for the dehydrated AER.

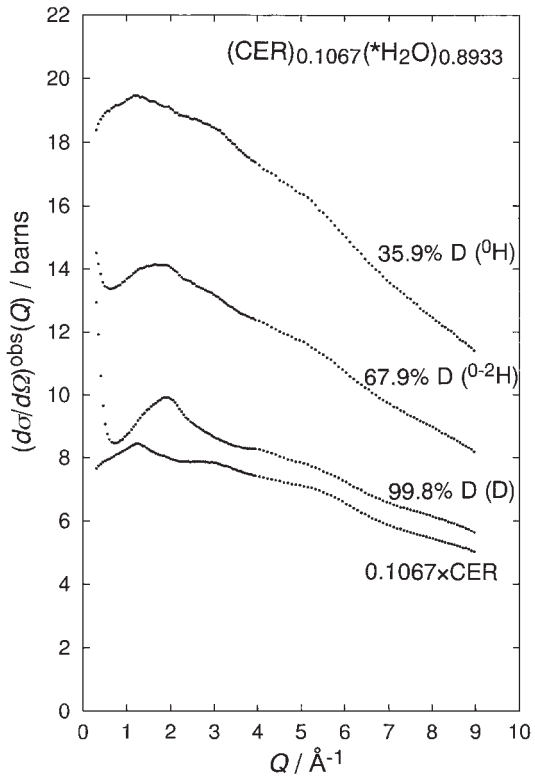

Fig. 2. Same notations as in Fig. 1, except for the cation exchange resin (CER) samples.

ated at 20 MW in the Japan Atomic Energy Research Institute (JAERI), Tokai, Japan. The incident neutron wavelength, $\lambda = 1.089 \pm 0.004$ Å, was determined by Bragg reflections from the KCl powder. Beam collimations were 40′–80′–80′ in going from the reactor to the detector. The aperture of the collimated beam was 20 mm in width and 40 mm in height. Scattered neutrons were collected over the angular range of $3 \leq 2\theta \leq 102°$, corresponding to the scattering vector magnitude range of $0.30 \leq Q \leq 8.97$ Å^{-1} ($Q = 4\pi \sin\theta/\lambda$). The step interval was chosen to be $\Delta 2\theta = 0.5°$ in the range of $3 \leq 2\theta \leq 40°$ and $\Delta 2\theta = 1°$ in the range of $41 \leq 2\theta \leq 102°$, respectively. The preset time was 180 s for each data point. Scattering intensities were measured in advance for the dehydrated AER and CER samples, empty cell, vanadium rod of 10 mm in diameter, and instrumental background.

Data Reduction. The measured scattering intensities were corrected for the background scattering, absorption of both the sample, and cell.[9] The corrected count rate of the sample was converted to the absolute scale by use of the corrected scattering intensity from the vanadium rod. The observed scattering cross sections for anion and cation exchange resins involving isotopically substituted water molecules are shown in Figs. 1 and 2, respectively. The scattering cross section observed for the wet resins involve contributions from the water–water, water–resin, and resin–resin interactions. In order to extract the water–water and water–resin interactions from the observed scattering cross section, it is necessary to remove the intra- and intermolecular interference contributions within the resin. In the present analysis, the observed scattering intensities from the dehydrated resins were multiplied by the mole fraction of the resin, x, defined by the stoichiometric representation, $(Resin)_x(^*H_2O)_{1-x}$, and then subtracted from those observed for the wet resins. The change in the microscopic structure in the divinylbenzene cross-linked ion exchange resins by

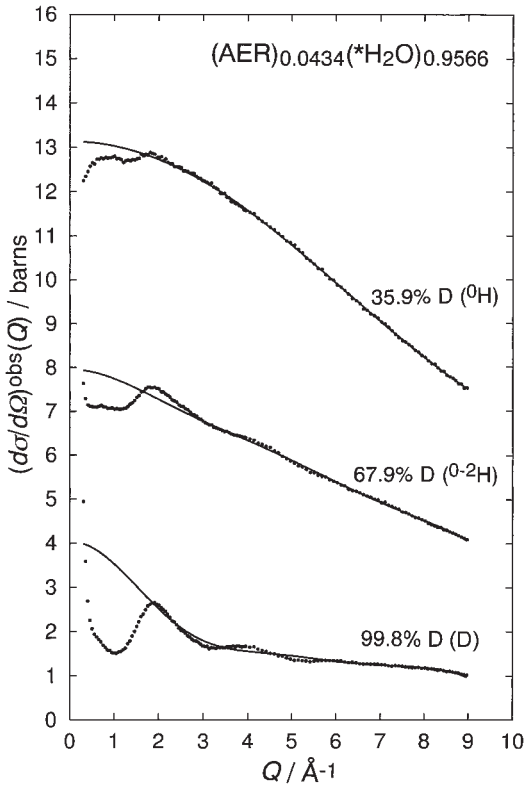

Fig. 3. Observed difference scattering cross sections for water molecules absorbed in the AER samples (dots) with different H/D ratios of exchangeable hydrogen atoms. Solid lines denote the sum of the intramolecular interference term of the water molecule in Eq. 2 and the self scattering term in Eq. 3.

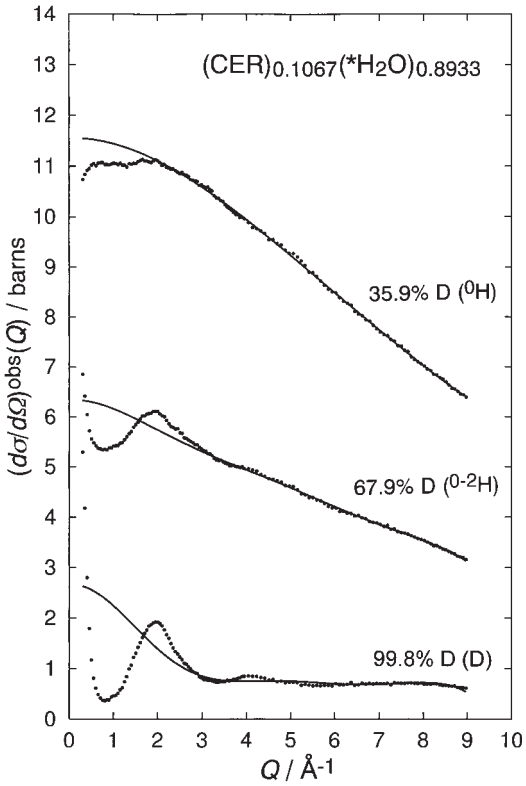

Fig. 4. Same notations as in Fig. 3, except for the cation exchange resin (CER) samples.

swelling has been proved to be negligibly small at least within the range of $r < 10$ Å,[3] where important short-range structural information on the nearest neighbor intermolecular interactions should be included. Furthermore, in the present experimental condition, the observed interference amplitude for the dehydrated resin seems to be relatively small compared to that for interference contribution from water molecules inside the resin as depicted in Figs. 1 and 2. Therefore, the short-range contribution within the resin is expected to be adequately subtracted by the procedure employed in the present analysis. The next step of the data analysis is to extract the intermolecular interference term for the samples.

Figures 3 and 4 represent the difference scattering cross sections observed for the AER and CER samples, respectively, after subtraction of the scattering intensities from the dehydrated resins. The difference scattering cross section consists of the contributions from the intramolecular interference term of the water molecule, the intermolecular interference term, and the self scattering term, i.e.,

$$(\mathrm{d}\sigma/\mathrm{d}\Omega)^{\mathrm{obs}} = (\mathrm{d}\sigma/\mathrm{d}\Omega)_{\mathrm{int}}{}^{\mathrm{intra}} + (\mathrm{d}\sigma/\mathrm{d}\Omega)_{\mathrm{int}}{}^{\mathrm{inter}} + (\mathrm{d}\sigma/\mathrm{d}\Omega)^{\mathrm{self}}. \quad (1)$$

The intramolecular interference term can be written as

$$(\mathrm{d}\sigma/\mathrm{d}\Omega)_{\mathrm{int}}{}^{\mathrm{intra}} = (1-x)[4b_{\mathrm{O}}b_{\mathrm{H}}\exp(-l_{\mathrm{OH}}{}^2Q^2/2)\sin(Qr_{\mathrm{OH}})/(Qr_{\mathrm{OH}}) + 2b_{\mathrm{H}}{}^2\exp(-l_{\mathrm{HH}}{}^2Q^2/2)\sin(Qr_{\mathrm{HH}})/(Qr_{\mathrm{HH}})], \quad (2)$$

where r_{ij} and l_{ij} denote the interatomic distance and the root mean square amplitude of the i–j pair, respectively.

The self scattering term in Eq. 1 certainly involves the inelasticity contribution, which is clearly observed in Figs. 3 and 4 as pronounced decreases in the intensities of the scattering cross section at the higher-Q region. Although several theoretical approaches have been proposed in the literature,[10–13] no general correction procedure seems to have been established for the multiple and inelasticity scattering corrections for the system containing a considerable amount of H atoms. Previous Monte-Carlo calculations have indicated that the observed scattering intensities in the liquid formic acid containing a large amount of H atoms depend considerably on Q, reflecting the strong Q-dependence of the multiple scattering term.[14] The intensities of difference scattering cross sections observed for the present samples also exhibit strong Q-dependent scattering intensities owing to the inelasticity effect of H. Since it is difficult to evaluate the multiple scattering contribution for the present sample adequately by a simple isotropic approximation of Blech and Averbach,[15] we employ in the present analysis the empirical method of the polynomial expansion, which has frequently been applied to the data correction for samples containing complexed molecules, such as liquid methanol,[16,17] ethanol,[18] and D-glycerol.[19] More recently, Belissent-Funel et al. have indicated that the polynomial expansion method supplies reliable inelasticity correction for liquid D_2O and also for the H_2O–D_2O mixtures.[20] This polynomial method was also successfully adopted in evaluation of the self scattering term observed for the $^*HCl$–$^*H_2O$[21] and the alanine–$^*H_2O$[22] systems. In the present analysis, the self term in Eq. 1 is evaluated by

$$(\mathrm{d}\sigma/\mathrm{d}\Omega)^{\mathrm{self}} = (\mathrm{d}\sigma/\mathrm{d}\Omega)^{\mathrm{coh}} + (\mathrm{d}\sigma/\mathrm{d}\Omega)^{\mathrm{inc}} + (\mathrm{d}\sigma/\mathrm{d}\Omega)^{\mathrm{multi}} = A + BQ^2 + CQ^4 + DQ^6 + EQ^8. \quad (3)$$

The intermolecular interference term $(d\sigma/d\Omega)_{int}^{inter}$ decays much faster against Q than the intramolecular interference term $(d\sigma/d\Omega)_{int}^{intra}$, because the former is composed of atomic pair correlations with larger interatomic distances and larger r.m.s. amplitudes. Then, the total $(d\sigma/d\Omega)^{obs}$ in the higher-Q region can be well approximated as the sum of the intramolecular and self scattering terms. Coefficients of the polynomial function A–E in Eq. 3 were determined by the least-squares fitting procedure under the condition of minimizing the value U defined below:

$$U = \int_{Q_{min}}^{Q_{max}} [(d\sigma/d\Omega)^{obs} - \alpha(d\sigma/d\Omega)_{int}^{intra} - (d\sigma/d\Omega)^{self}]^2 dQ. \quad (4)$$

The upper limit Q_{max} was set to 8.97 Å^{-1}, the maximum value of the present observed data. The lower limit Q_{mim} was chosen to be 3.0 Å^{-1} in the present analysis, considering the following criteria in determining a reliable $(d\sigma/d\Omega)_{int}^{inter}$ term:

1) Amplitude of the intermolecular interference term should be small in the Q-region above the Q_{min}.

2) The values of the intermolecular distribution function, calculated by the Fourier transform of the $(d\sigma/d\Omega)_{int}^{inter}$ in the lower-r region between $r = 0$ to 1.5 Å, is minimized.

In the fitting procedure, the renormalization factor α in Eq. 4 and the intramolecular parameter r_{OH} in Eq. 2 were treated as independent parameters in order to check the reliability of the present correction procedure. The intramolecular parameters for the water molecule except for the r_{OH} were taken from values determined by neutron diffraction studies for liquid pure D_2O.[23,24] The fitting procedure was performed by the SALS program.[25] The value of r_{OH} determined was 0.98(1) Å for AER–D_2O, AER–$^{0-2}H_2O$, CER–D_2O, and CER–$^{0-2}H_2O$ samples. The value is in complete agreement with that determined by neutron diffraction studies for liquid pure D_2O.[23,24] The values for the renormalization factor $\alpha = 0.97(1)$ and 0.98(1) were obtained for the AER–D_2O and AER–$^{0-2}H_2O$ samples, respectively. The values $\alpha = 0.98(1)$ and 1.00(1) were determined for the CER–D_2O and CER–$^{0-2}H_2O$ samples, respectively. These results imply that the uncertainties in the data normalization are estimated below ca. 3% in the present analysis. Consequently, the intermolecular interference term, $(d\sigma/d\Omega)_{int}^{inter}$, was evaluated by the following equation:

$$(d\sigma/d\Omega)_{int}^{inter} = (d\sigma/d\Omega)^{obs} - (d\sigma/d\Omega)_{int}^{intra} - (d\sigma/d\Omega)^{self}. \quad (5)$$

Intermolecular partial structure factors, $a_{HH}(Q)$, $a_{XH}(Q)$, and $a_{XX}(Q)$ (X: atoms involved in the sample except for the water hydrogen), were deduced from the combination of observed $(d\sigma/d\Omega)_{int}^{inter}$ terms for the three samples involving D_2O, ^0H_2O, and $^{0-2}H_2O$:

$$(d\sigma/d\Omega)_{int}^{inter}\ (\text{for D}) + (d\sigma/d\Omega)_{int}^{inter}\ (\text{for } ^0\text{H}) - 2(d\sigma/d\Omega)_{int}^{inter}\ (\text{for } ^{0-2}\text{H}) = 2(1-x)^2 b_D^2 [a_{HH}(Q) - 1], \quad (6)$$

$$4(d\sigma/d\Omega)_{int}^{inter}\ (\text{for } ^{0-2}\text{H}) - (d\sigma/d\Omega)_{int}^{inter}\ (\text{for D}) - 3(d\sigma/d\Omega)_{int}^{inter}\ (\text{for } ^0\text{H}) = 4x(1-x) b_R b_D [a_{RH}(Q) - 1] + 4(1-x)^2 b_O b_D [a_{OH}(Q) - 1] = 4(1-x) b_D [x b_R + (1-x) b_O][a_{XH}(Q) - 1], \quad (7)$$

$$(d\sigma/d\Omega)_{int}^{inter}\ (\text{for } ^0\text{H}) = 2x(1-x) b_R b_O [a_{RO}(Q) - 1] + (1-x)^2 b_O^2 [a_{OO}(Q) - 1] = (1-x) b_O [2x b_R + (1-x) b_O][a_{XX}(Q) - 1], \quad (8)$$

where b_R stands for the sum of the coherent scattering lengths of atoms involved in the average monomeric unit of the resin. Partial structure factors $a_{RH}(Q)$ and $a_{RO}(Q)$ represent the interference contributions between atoms involved in the resin and water-hydrogen and water-oxygen atoms, respectively.

The intermolecular distance, the root-mean-square displacement, and the coordination number, r_{ij}, l_{ij}, and n_{ij}, for the i–j pair were determined by a least-squares fit of the observed intermolecular partial structure factors to the corresponding calculated ones, $a_{ij}^{calc}(Q)$, which involve a contribution from the long-range random distribution of atoms as follows:[26–28]

$$a_{ij}^{calc}(Q) = \sum \beta_{ij} n_{ij} \exp(-l_{ij}^2 Q^2/2) \sin(Q r_{ij})/(Q r_{ij}) + 4\pi\rho \exp(-l_0^2 Q^2/2)[Q r_0 \cos(Q r_0) - \sin(Q r_0)] Q^{-3}, \quad (9)$$

where ρ is the number density of the stoichiometric unit $(Resin)_x$-$(^*H_2O)_{1-x}$. The parameter r_0 denotes the distance beyond which the uniform distribution of atoms is assumed, and l_0 describes the sharpness of the boundary at r_0. The coefficient β_{ij} in Eq. 9 is given as

$$\beta_{HH} = (1-x)^{-1}/2, \quad (10)$$

$$\beta_{OH} = b_O [x b_R + (1-x) b_O]^{-1}/2, \quad (11)$$

and

$$\beta_{OO} = b_O [2x b_R + (1-x) b_O]^{-1}. \quad (12)$$

Since the present intermolecular partial structure factors $a_{XH}(Q)$ and $a_{XX}(Q)$ contain interactions between atoms consisting the resin and those within the water molecule, it is generally difficult to distinguish contributions from the water–water and water–resin interactions. In the present least-squares fitting analysis, the short-range interactions in $a_{XH}(Q)$ and $a_{XX}(Q)$ are treated as the O–H and O–O interactions, respectively. Structural parameters obtained in the present analysis are therefore regarded as the average values containing contributions from both the water–water and resin–water interactions. The fitting procedure was made in the range of $0.30 \le Q \le 8.97$ Å^{-1} using the SALS program.[25]

The intermolecular partial distribution function $g_{ij}(r)$ is represented as the Fourier transform of the observed $a_{ij}(Q)$:

$$g_{ij}(r) = 1 + (2\pi^2 \rho r)^{-1} \int_0^{Q_{max}} Q[a_{ij}(Q) - 1] dQ. \quad (13)$$

The upper limit Q_{max} of the integral was taken to be 8.97 Å^{-1}. Although the present value of the Q_{max} is relatively small to reproduce a short-range structural feature with sufficient r-space resolution, the calculated $g_{ij}(r)$ should be useful for checking the consistency between the calculated short-range structure derived from the least-squares refinement and that from the observed $a_{ij}(Q)$.

Results and Discussion

Anion Exchange Resin (AER). The observed intermolecular interference term, $(d\sigma/d\Omega)_{int}^{inter}$, for the AER samples preferably oscillates around the asymptotic value 0 as shown in Fig. 5. This implies that the polynomial fit applied for evaluation of the self scattering term has been adequately carried out. A marked difference in the interference feature between the $(d\sigma/d\Omega)_{int}^{inter}$ for these samples is attributable to the difference in the average coherent scattering length of water-hydrogen atoms.

Intermolecular partial structure factors for the AER sample, $a_{HH}(Q)$, $a_{XH}(Q)$, and $a_{XX}(Q)$, were obtained by the combination of the observed $(d\sigma/d\Omega)_{int}^{inter}$ through Eqs. 6–8, which

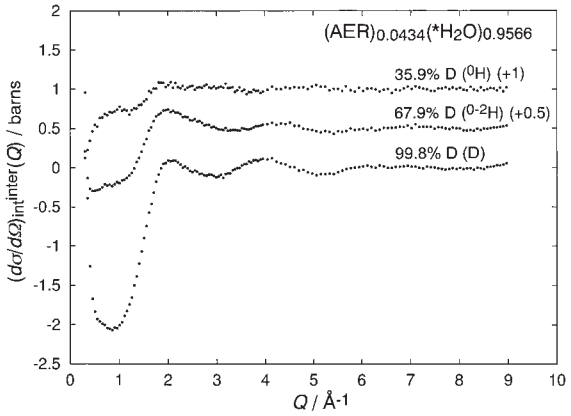

Fig. 5. Observed intermolecular interference term for the AER samples with different H/D ratios (dots).

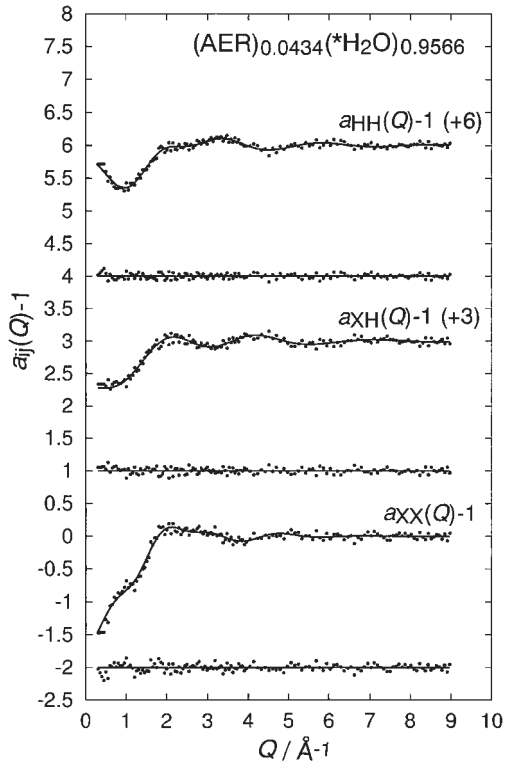

Fig. 6. Dots: Observed intermolecular H–H, X–H, and X–X partial structure factors, $a_{ij}(Q)$, for the AER samples. Solid lines: The best-fit of calculated interference term in Eq. 9. The difference between observed and calculated $a_{ij}(Q)$ is shown below (dots).

are given in Fig. 6. Corresponding intermolecular distribution functions $g_{ij}(r)$, for the AER sample, are shown in Fig. 7. The structural parameters, r_{ij}, l_{ij}, and n_{ij}, were determined by the least-squares fit to the observed $a_{ij}(Q)$ using the theoretical function in Eq. 9, which involves short- and long-range contributions. Prior to the fitting procedure, the correction for the low-frequency systematic errors in the observed $a_{ij}(Q)$ was applied.[24] In the present fitting, it was assumed that statistical uncertainties distribute uniformly over the whole range of Q. Contributions from the first and second nearest neighbor interactions were taken into account in evaluating the present theoretical $a_{ij}(Q)$.

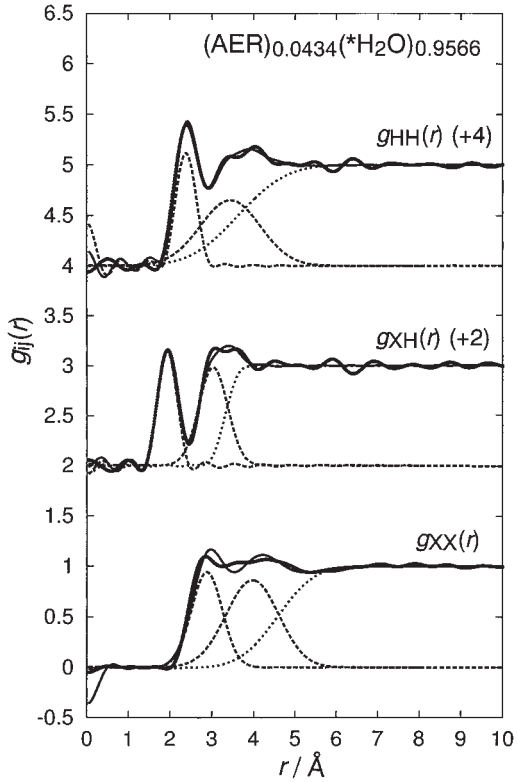

Fig. 7. Thick solid lines: Observed intermolecular H–H, X–H, and X–X partial distribution functions, $g_{ij}(r)$, for the AER samples. Thin solid lines: The Fourier transform of the calculated $a_{ij}(Q)$, presented as the solid lines in Fig. 6. Contributions from the short- and long-range interactions are denoted by broken and dotted lines, respectively.

The results of the least-squares refinements are summarized in Table 2. The nearest neighbor H···H distance, $r_{HH} = 2.40(3)$ Å, observed for the AER sample is in excellent agreement with that reported for pure liquid water.[21,29–34] The present nearest neighbor O···H distance ($r_{OH} = 1.95(3)$ Å) is slightly longer than that for pure water (1.85 Å),[30,34] while it is in good agreement with those observed for aqueous 8 mol % NH_4Cl ($r_{OH} =$ 1.91 Å),[35] 10 mol % LiBr ($r_{OH} = 1.91$ Å),[36] and 2.5 mol % DL-alanine ($r_{OH} = 1.90$ Å)[22] solutions. The value of the present nearest neighbor O···H coordination number in the AER sample was determined to be 1.8(1), which agrees well with that reported for pure water ($n_{OH} = 1.8$).[30] These results imply that the hydrogen-bonded structure among water molecules in AER is very similar to that in the pure liquid water. On the other hand, the present value of the nearest neighbor O···O distance, $r_{OO} = 2.93(5)$ Å, is considerably larger than that for pure water. It may be considered that the other interactions between the water-oxygen and methyl-hydrogen and -carbon atoms of the trimethylammonium group within the ion exchange site of the AER are overlapped in this region. The intermolecular distance between the methyl-hydrogen atom and the nearest neighbor water-oxygen atom has been reported to be 2.58 Å for an aqueous 3 mol % DL-alanine solution.[37] This methyl-hydrogen and water-oxygen interaction may contribute as a

Table 2. Results of the Least-Squares Refinement for Partial Structure Factors, $a_{HH}(Q)$, $a_{XH}(Q)$, and $a_{XX}(Q)$, Observed for $(AER)_{0.0434}(^*H_2O)_{0.9566}$ and $(CER)_{0.1067}(^*H_2O)_{0.8933}$[a)]

		$(AER)_{0.0434}(^*H_2O)_{0.9566}$			$(CER)_{0.1067}(^*H_2O)_{0.8933}$		
		$a_{HH}(Q)-1$	$a_{XH}(Q)-1$	$a_{XX}(Q)-1$	$a_{HH}(Q)-1$	$a_{XH}(Q)-1$	$a_{XX}(Q)-1$
	i–j	H–H	O–H	O–O	H–H	O–H	O–O
1st nearest	r_{ij}/Å	2.40(3)	1.95(3)	2.93(5)	2.28(3)	1.78(3)	2.80(3)
Neighbor	l_{ij}/Å	0.22(3)	0.20(3)	0.36(3)	0.19(3)	0.15(3)	0.23(3)
	n_{ij}	2.43(3)	1.8(1)	3.4(8)	1.3(1)	1.0(1)	2.4(1)
2nd nearest	r_{ij}/Å	3.59(3)	3.07(5)	4.1(1)	3.27(8)	3.3(5)	4.19(5)
Neighbor	l_{ij}/Å	0.70(3)	0.34(5)	0.6(1)	0.78(3)	0.58(3)	0.72(3)
	n_{ij}	9(1)	6(1)	10(5)	4.7(8)	8(1)	12(1)
Long-range	r_0/Å	3.84(8)	3.3(1)	4.7(8)	3.2(1)	3.4(1)	5.1(1)
Interaction	l_0/Å	0.88(5)	0.2(1)	0.7(5)	0.60(8)	0.6(3)	0.60(5)

a) Estimated errors are given in the parentheses.

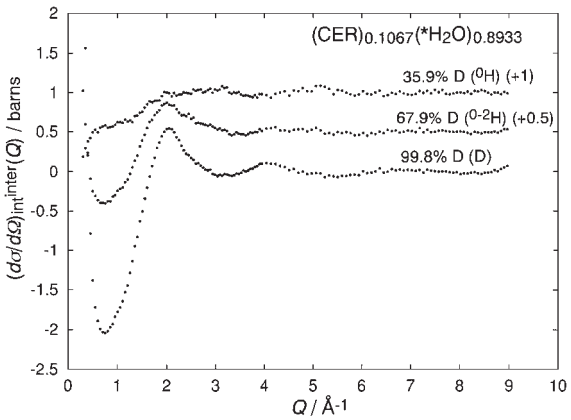

Fig. 8. Same notations as in Fig. 5, except for the CER samples.

negative peak in the present $g_{XX}(r)$ because of the negative scattering length of the H atom. This will cause the position of the average intermolecular interaction of the $g_{XX}(r)$ to be more distant.

Cation Exchange Resin (CER). The observed intermolecular interference term, $(d\sigma/d\Omega)_{int}^{inter}$, for the CER samples is represented in Fig. 8. A systematic difference in the interference feature of $(d\sigma/d\Omega)_{int}^{inter}$ can be observed according to the difference in the average scattering length of the water-hydrogen atom. Intermolecular partial structure factors, $a_{HH}(Q)$, $a_{XH}(Q)$, and $a_{XX}(Q)$, for the CER sample were derived by combining the observed $(d\sigma/d\Omega)_{int}^{inter}$ by applying Eqs. 6–8, as shown in Fig. 9. Corresponding intermolecular partial distribution functions are given in Fig. 10. The first peak located at $r \approx 2.3$ Å in the present $g_{HH}(r)$ is attributable to the nearest neighbor intermolecular H···H interaction between hydrogen-bonded water molecules; however, the position is ca. 0.1 Å shorter than that observed for pure water and water absorbed in the AER sample as described above. The position of the first peak appearing at $r \approx 1.8$ Å in the present $g_{XH}(r)$, is slightly shorter than that for the hydrogen-bonded O···H correlation in pure liquid water. The height of this nearest neighbor peak is considerably lower than that found in pure water. This implies that the hydrogen-bonded structure within the CER sample is significantly different from that in pure liquid water.

The results of the least-squares refinements are represented

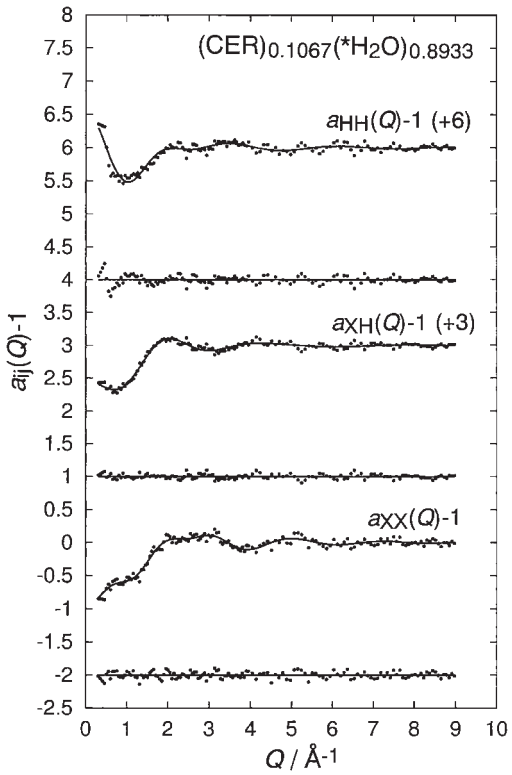

Fig. 9. Same notations as in Fig. 6, except for the CER samples.

in Table 2. The nearest neighbor H···H distance in the CER sample (2.28(3) Å) is ca. 0.1 Å shorter than that reported for pure liquid water (2.4 Å).[21,29–34] The present value of the nearest neighbor O···H distance (1.78(3) Å) is also considerably shorter than that for pure water. The nearest neighbor O···H coordination number was obtained to be 1.0(1), indicating that the hydrogen-bonded network among water molecules is significantly affected by the presence of the sulfonate group in the CER. According to our previous neutron diffraction study on concentrated aqueous sulfuric acid solutions, a considerably shorter O···H distance, $r_{O\cdots H} = 1.7$ Å, was observed,[38] which reflects strong intermolecular hydrogen bonds. The shorter O···H distance has also been found in highly concentrated aqueous hydrochloric acid solutions ($r_{O\cdots H} = 1.69$ Å),[21] which

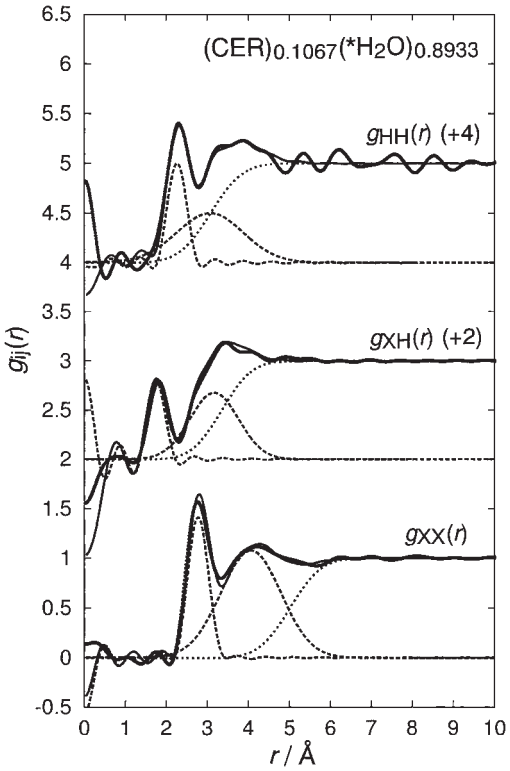

Fig. 10. Same notations as in Fig. 7, except for the CER samples.

is strongly related with the O···H distance within the protonated water dimer, $H_5O_2^+$. The present value of the nearest neighbor O···H distance (1.78(3) Å) can be regarded as the average value of the short O···H distance closely related with $H_5O_2^+$ and the normal hydrogen-bonded distances among water molecules. These results indicate that the intermolecular hydrogen-bonded structure among water molecules is significantly modified due to the strongly acidic environment in the CER sample.

The authors wish to thank Professor Kazuma Hirota (ISSP, the University of Tokyo) for his help during the course of neutron diffraction measurements. We are grateful to Professor Hideki Yoshizawa (ISSP, the University of Tokyo) and Mr. Yoshihisa Kawamura (ISSP, the University of Tokyo) for their stimulating discussions and encouragement. All calculations were carried out at the Yamagata University Networking and Computing Service Center. This work was partially supported by a Grant-in-Aid for Scientific Research on Priority Areas (No. 16041205), Scientific Research (C) (No. 16550049) and Creative Scientific Research (No. 16GS0417) from the Ministry of Education, Culture, Sports, Science and Technology.

References

1 *Ion Exchange Technology*, ed. by D. Naden, M. Streat, Ellis Horwood Limited, West Sussex, England, **1984**.

2 *Ion Exchange for Industry*, ed. by M. Streat, Ellis Horwood Limited, West Sussex, England, **1988**.

3 F. Ikkai, M. Shibayama, *J. Polym. Sci., Part B: Polym. Phys.* **1996**, *34*, 1637.

4 R. H. Tromp, G. W. Neilson, *J. Phys. Chem.* **1996**, *100*, 7380.

5 T. Okada, M. Harada, *Anal. Chem.* **2004**, *76*, 4564.

6 V. F. Sears, *Neutron News* **1992**, *3*, 26.

7 J. G. Powles, *Adv. Phys.* **1973**, *22*, 1.

8 J. R. Granada, V. H. Gillete, R. E. Mayer, *Phys. Rev. A* **1987**, *36*, 5594.

9 H. H. Paalman, C. J. Pings, *J. Appl. Phys.* **1962**, *33*, 2635.

10 G. Placzek, *Phys. Rev.* **1952**, *86*, 377.

11 J. G. Powles, *Mol. Phys.* **1979**, *37*, 623.

12 M. Rovere, L. Blum, A. H. Narten, *J. Chem. Phys.* **1984**, *73*, 3729.

13 J. R. Granada, *Phys. Rev. B* **1985**, *31*, 4167.

14 H. Bertagnolli, P. Cheux, H. G. Hertz, *Ber. Bunsen-Ges. Phys. Chem.* **1984**, *88*, 977.

15 I. A. Blech, B. L. Averbach, *Phys. Rev.* **1965**, *137*, A1113.

16 D. G. Montague, I. P. Gibson, J. C. Dore, *Mol. Phys.* **1981**, *44*, 1355.

17 D. G. Montague, J. C. Dore, *Mol. Phys.* **1986**, *57*, 1035.

18 D. G. Montague, I. P. Gibson, J. C. Dore, *Mol. Phys.* **1982**, *47*, 1405.

19 D. C. Champeney, R. N. Joarder, J. C. Dore, *Mol. Phys.* **1986**, *58*, 337.

20 M.-C. Bellissent-Funel, L. Bosio, J. Texeira, *J. Phys.: Condens. Matter* **1991**, *3*, 4065.

21 Y. Kameda, T. Usuki, O. Uemura, *Bull. Chem. Soc. Jpn.* **1998**, *71*, 1305.

22 Y. Kameda, M. Sasaki, M. Yaegashi, Y. Amo, T. Usuki, *Bull. Chem. Soc. Jpn.* **2004**, *77*, 1807.

23 J. G. Powles, *Mol. Phys.* **1981**, *42*, 757.

24 Y. Kameda, O. Uemura, *Bull. Chem. Soc. Jpn.* **1992**, *65*, 2021.

25 T. Nakagawa, Y. Oyanagi, *Recent Development in Statistical Inference and Data Analysis*, ed. by K. Matusita, North-Holland, **1980**, p. 221.

26 A. H. Narten, M. D. Danford, H. A. Levy, *Discuss. Faraday Trans.* **1967**, *43*, 97.

27 R. Caminiti, P. Cucca, M. Monduzzi, G. Saba, G. Crisponi, *J. Chem. Phys.* **1984**, *81*, 543.

28 H. Ohtaki, N. Fukushima, *J. Solution Chem.* **1992**, *21*, 23.

29 A. K. Soper, R. N. Silver, *Phys. Rev. Lett.* **1982**, *49*, 471.

30 A. K. Soper, M. G. Phillips, *Chem. Phys.* **1986**, *107*, 47.

31 A. K. Soper, *Chem. Phys.* **1986**, *107*, 61.

32 A. K. Soper, *J. Chem. Phys.* **1994**, *101*, 6888.

33 P. Postrino, M. A. Ricci, A. K. Soper, *J. Chem. Phys.* **1994**, *101*, 4133.

34 A. K. Soper, F. Bruni, M. A. Ricci, *J. Chem. Phys.* **1997**, *106*, 247.

35 Y. Kameda, K. Sugawara, T. Usuki, O. Uemura, *J. Phys. Soc. Jpn.* **2001**, *70*, Suppl. A, 362.

36 Y. Kameda, M. Imano, M. Takeuchi, S. Suzuki, T. Usuki, O. Uemura, *J. Non-Cryst. Solids* **2001**, *293–295*, 600.

37 Y. Kameda, K. Sugawara, T. Usuki, O. Uemura, *Bull. Chem. Soc. Jpn.* **2003**, *76*, 935.

38 Y. Kameda, K. Hosoya, S. Sakamoto, H. Suzuki, T. Usuki, O. Uemura, *J. Mol. Liq.* **1995**, *65/66*, 305.